Appl. Phys. B (2013) 112:479–484
DOI 10.1007/s00340-013-5600-5

Applied Physics B
Lasers and Optics

RAPID COMMUNICATION

# Programmable all-fiber structured waveshaper based on linearly chirped fiber Bragg grating and digital thermal controller

**Hailiang Zhang · Ming Tang · Yiwei Xie · Huiqi Liao · Songnian Fu · Perry Ping Shum · Deming Liu**

Received: 11 July 2013 / Accepted: 24 July 2013 / Published online: 10 August 2013


**Abstract** We proposed and experimentally demonstrated an all-fiber structured programmable optical bandpass filter (waveshaper) based on a linearly chirped fiber Bragg grating and a digital-controlled thermal array. The key parameters of this filter such as the number of transmission channels, passing bandwidth per channel, central wavelength as well as the channel spacing can be reconfigured independently and flexibly by a program-controlled circuit. We have achieved in experiments the tunable passing bandwidth ranging from $< 0.04$ to 1.55 nm, adjustable central wavelength ranging from 1,547.16 to 1,558.64 nm, and a minimum wavelength spacing of 0.91 nm. The insertion loss of the whole device and the sideband rejection ratio are about 1.76 and 28 dB, respectively.

## 1 Introduction

Along with the rapid development of optical communication systems, there is a transition from static to reconfigurable architecture to provide flexible bandwidths and wavelengths for dynamically allocating spectral resources and maximizing transmission efficiency. As the key elements in the flex-grid supported optical network, tunable optical filters (TOFs) are required to be smart enough for adjusting the quantity of channels, central wavelengths, wavelength spacing, and channel bandwidth independently [1–3]. For fulfilling the stringent requirements, currently optical filters based on Liquid Crystal on Silicon (LCoS) technology has been employed to provide flexible filtering functions in the market, such as the waveshaper designed and produced by Finisar. However, as this type of TOF consists of discrete optical elements and free-space coupling modules, it suffers from bulky structure, high cost, and large insertion loss (typically $> 4.5$ dB) [4]. To minimize the insertion loss and system's cost, it is favorable to apply the all-fiber structure, and the linearly chirped fiber Bragg grating (LCFBG) with wide optical bandgap in telecommunication window is a good candidate to achieve waveshaper functions without any moving parts.

Although the LCFBG exhibits wide stop band in its transmission direction, it is well known that a phase shift of $\pi$ can result in a transmission window in the stop band [5]. Therefore, to develop the above mentioned TOFs, a temporary phase shift of $\pi$ should be introduced into LCFBG by applying external field (either stress or temperature). As an example of stress-induced phase-shift, mini-size piezoelectric transducers (PZTs) are used to induce temporary phase shifts in LCFBG [6, 7]. However, this method cannot tune the center wavelength continuously, and the wavelength spacing is limited by the physical size of PZT elements. For the temperature-induced phase shift, narrow resistance wires are used to heat the local region of LCFBG [8–11]. However, this method results in low response speed, unpredictable repeatability of wavelength positioning, and poor stability against environmental interferences. As an improvement of the thermal effect-controlled phase shift, Petermann

H. Zhang · M. Tang (✉) · Y. Xie · H. Liao · S. Fu · P. P. Shum · D. Liu
National Engineering Laboratory for Next Generation Internet Access System (NGIA), School of Optical and Electronic Information and Wuhan National Laboratory for Optoelectronics (WNLO), Huazhong University of Science and Technology, Wuhan 430074, China
e-mail: tangming@mail.hust.edu.cn

P. P. Shum
School of EEE, Nanyang Technological University, 50 Nanyang Avenue, Singapore 639798, Singapore

et al. [12] demonstrated a tunable optical bandpass filter by replacing the heating resistance wires with a thermal printhead (TPH). There are many advantages of using a TPH to induce a temporary phase shift in the LCFBG, such as fast response speed ($\sim$ millisecond), accurate repeatability of wavelength positioning, compact size, and its programmable capability to establish simple and flexible operations. However, only fixed passing bandwidth has been achieved in this type of TOF, and further work needs to be explored to accomplish the flexible waveshaper performance.

In this paper, we utilize a TPH to heat a LCFBG at one or multiple arbitrarily designed local regions, and demonstrate a flexible-grid compatible bandpass filter that is able to tune the number of channels, passing bandwidth, center wavelengths, and wavelength spacing independently. The transmission bandwidth can be adjusted from 0.035 to 1.55 nm, the central wavelength of the transmission peak can be shifted continuously from 1,547.16 to 1,558.64 nm, and the minimum wavelength spacing between each channel is 0.91 nm. The minimum insertion loss of the device is about 1.76 dB, and the sideband suppression ratio has been achieved to be 28 dB, respectively.

## 2 Principle and system diagram

### 2.1 Principle of filtering effect based on LCFBG

The local Bragg wavelength along the LCFBG can be given by:

$$\lambda(z) = 2n_{\text{eff}}\Lambda(z) \tag{1}$$

where $n_{\text{eff}}$ is the core effective refractive index, $\Lambda(z)$ is the local grating period, and $z$ represents the location along the LCFBG. Equation (1) indicates that the local Bragg wavelength changes linearly with the position along the LCFBG axis.

By heating the LCFBG, the core effective refractive index and the local grating period in the heated region will be changed. The changes can be written as the following two equations, respectively:

$$\Delta n_{\text{eff}} = \beta \Delta T n_{\text{eff}} \tag{2}$$

$$\Delta\Lambda = \alpha \Delta T \Lambda(z) \tag{3}$$

where $\Delta T$ is the temperature change, $\beta$ is the thermal optical coefficient, and $\alpha$ is the thermal expansion coefficient. For silica, $\beta$ and $\alpha$ are about $8.6 \times 10^{-6}$/ °C and $5.5 \times 10^{-7}$/ °C, respectively. Since $\beta$ is much higher than $\alpha$, the thermal expansion effect can be neglected [13]. A temporary phase shift will be introduced into the heating local region when the LCFBG is heated, and the phase shift value is determined by

$$\Delta\Phi = \frac{2\pi L}{\lambda_B(z)} \Delta n_{\text{eff}} \tag{4}$$

Here, $L$ is the heating width. According to Eqs. (2) and (4), it can be rewritten as

$$\Delta\Phi = \frac{2\pi L}{\lambda} \beta \Delta T n_{\text{eff}} \tag{5}$$

When the temperature change is large enough, a phase shift of $\pi$ will be introduced into the LCFBG and a narrow transmission peak will be generated within the stop band. In addition, the bandwidth of the transmission peaks can be tuned by optimizing the heating strategy. As the local Bragg wavelength changes linearly with the position along the LCFBG axis, the number and central wavelength of the transmission peaks are determined by the quantity and the position of the heated local points, respectively.

### 2.2 Experimental configurations

Any standard TPH can be utilized as the heating device. The TPH we used in this work is FTP-628MCL701, manufactured by Fujitsu. This TPH has a 48 mm long heating array that consists of 384 heating elements, and thus, the element pitch is 0.125 mm. Each of the heating elements can work independently, which means that arbitrary local position of the LCFBG can be heated accurately assuming good contact. As the heating elements are fairly dense and tiny in physical size, it is hard to accurately measure the temperature rise caused by the activated heating elements. The heating is controlled by the duty ratio of the driving electrical pulse, and the dissipated power varies with that. The best experimental results can be obtained through adjusting the duty ratio. In our experiments, the average dissipated power of each heating element is about 100 mW. Because the intrinsic switching response time of heating elements is $< 2$ ms, and the on–off time of filtering is $< 1$ s, respectively, the transmission channels of this optical filter can be reconfigured quickly.

Principle of the proposed flexible waveshaper is schematically shown in Fig. 1a. A 75 mm long LCFBG is fixed tightly on the heating array of a TPH. Figure 1b shows the system diagram of the experiments. The amplified spontaneous emission (ASE) of a semiconductor optical amplifier (SOA) is used as the broadband light source (BLS). Due to heat diffusion, the temperature of the LCFBG's unheated region around the heating local region also increases. Since LCFBG's spectrum is susceptible to temperature change, this unwanted heat diffusion will result in broad perturbations of the grating's spectrum in the short-wavelength range [10]. A heat sink placed along

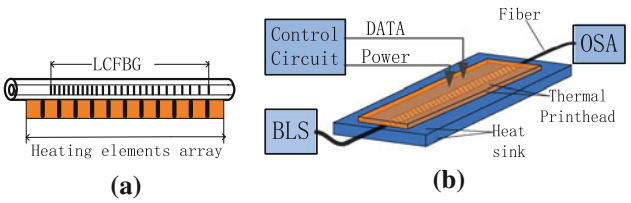


**Fig. 1** The proposed flex-tunable optical filter. **a** Schematic diagram. **b** Experimental setup

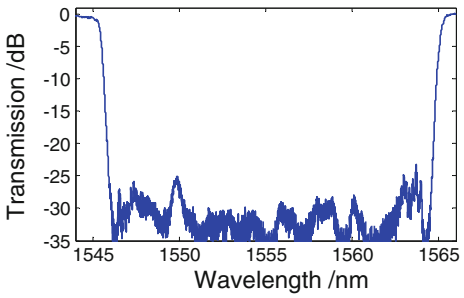


**Fig. 2** Transmission spectrum of the LCFBG without heating

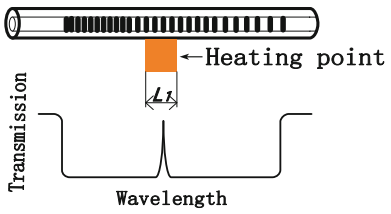


**Fig. 3** Principle of single transmission peak filtering

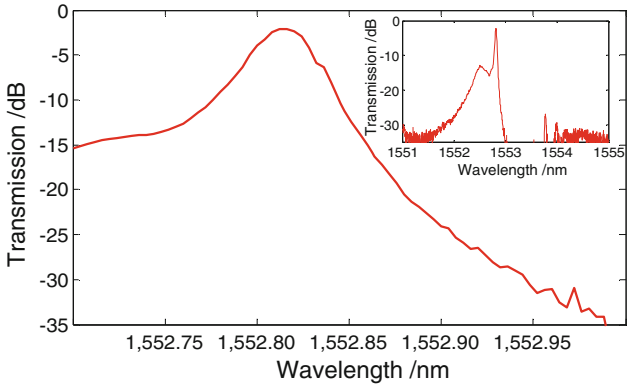


**Fig. 4** Transmission spectrum for 1.000 mm heater width

the LCFBG axis can alleviate this heat-diffusion-induced negative effect. The output of this filter is measured by using an optical spectrum analyzer (OSA), which has a best resolution of 0.02 nm. The TPH is connected to a micro-controller-based circuit, which dominates the heating elements array in a programmable way. Therefore, arbitrary local regions of the LCFBG can be heated in order to map our target spectrum. A flexible all-fiber structured waveshaper can be achieved to configure the number of channels, bandwidths, central wavelengths, and wavelength spacing independently.

In the experiments, the spectrum flatness of the SOA's ASE spectrum between 1,544 and 1,566 nm is about 0.89 dB when the driving current is set to 180 mA. The LCFBG has an approximately 25–30 dB deep stop band from 1,546.5 to 1,564.5 nm, as shown in the Fig. 2.

## 3 Experimental results

### 3.1 Single wavelength filtering performance

As illustrated in Fig. 3, when a local region of the LCFBG is heated, a transmission peak will be generated in the corresponding place of the stop band. $L_1$ is the heating width. When $L_1$ is set as 1.000 mm, which means that 8 consecutive heating elements work at the same time, a transmission peak is obtained within the stop band, as plotted in Fig. 4. The inset in Fig. 4 shows wider transmission spectrum between 1,551 and 1,555 nm. The transmission peak has a 3-dB bandwidth of $< 0.04$ nm, and the sideband rejection ratio is about 28 dB. There was a wide spectral perturbation in the shorter wavelength side of the transmission peak, and this was caused by the heat diffusion and the local Bragg wavelength shift. If the heating width is $< 1.000$ mm, the rejection ratio will decrease and the 3-dB bandwidth will increase, because the temperature change in the heated local region will be not enough to produce $\pi$ phase shift. In addition, the 3-dB bandwidth of the transmission peak will also increase if the heating width is wider than 1.000 mm.

By scanning the heating region without moving any components, we measure the central wavelengths of transmission channel while shifting the heating positions along the LCFBG. With 6 consecutive elements in one heating region, we sample the LCFBG by the interval of 5 heating elements. The obtained transmission peaks range from 1,547.16 to 1,558.64 nm and can be well fitted with a linear relationship, as shown in Fig. 5. The fitted equation is given by:

$$y = a * x + 1,558.87 \quad (6)$$

Here, $a$ represents the slope of the line, it is $-0.32$ nm/mm, $x$ is the heating position along the LCFBG axis, and $y$ is the central wavelength of the transmission peaks. The units of $x$ and $y$ are mm and nm, respectively. The linearity of the equation is fairly high with $R^2$ value of about 0.9997 ($R^2$ indicates the degree of the linearity for fitting the sampling values through linear fitting). In experiments, a tuning range of approximately 11.48 nm is obtained, and it

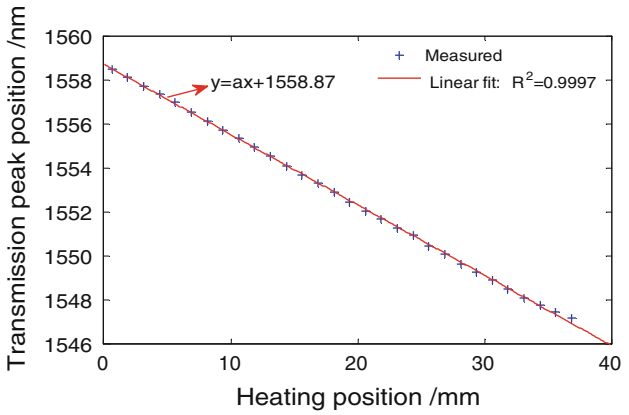


**Fig. 5** Relationship between the transmission peak position and heating position

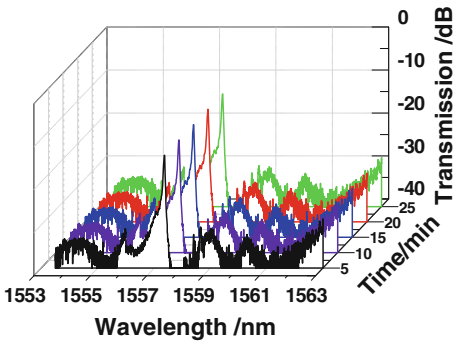


**Fig. 6** Transmission spectrum measured every 5 min

is only limited by the length of LCFBG and TPH (the length of the heating array used here is shorter than that of the LCFBG). Using a LCFBG with a wider stop band and a TPH with longer heating array will further improve the tuning range easily.

We also conducted long-term stability test for the filter by measuring the transmission spectrum every 5 min when the heater width is kept as 1.000 mm, as shown in Fig. 6. Reproducible transmission spectrum with good stability can be obtained without any change in the peak transmitivity and the central wavelength at the precision level of 0.02 nm. The fluctuation of ambient temperature can be neglected because the ambient temperature is much lower than that of the heating region.

### 3.2 Bandwidth tunability

In principle, the bandwidth of one transmission peak can be adjusted by changing the width of the heated local region. Since the Bragg wavelength at heating point may also shift with temperature, there will be an upper limit of bandwidth adjustment using one point heating strategy as the phase shift criteria described in Eq. (5) will be invalid. In

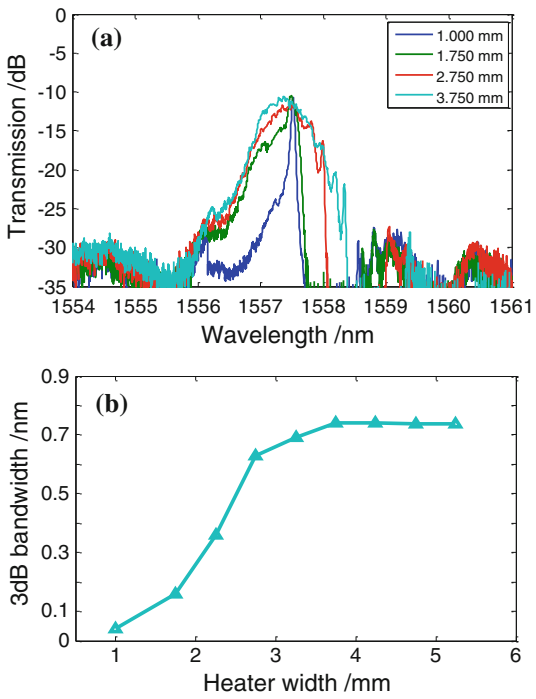


**Fig. 7** **a** Transmission spectrum for different heater widths. **b** 3-dB bandwidth of the transmission peak with respect to the heater width

experiments, different values of $L_1$ are set to heat the LCFBG, respectively. The transmission spectrum with different 3-dB bandwidth can be obtained, as illustrated in Fig. 7a. The relationship between 3-dB bandwidth of the transmission peak and the heating width $L_1$ is plotted in Fig. 7b. As predicted, the bandwidth can be broadened with the increases IN $L_1$ initially. However, the slope becomes flattened with further increasing $L_1$. When $L_1$ is wider than 3.750 mm, the bandwidth cannot be further broadened. The transmission peak has a maximum 3-dB bandwidth of about 0.74 nm with $L_1 = 3.750$ mm. Hence, the bandwidth can be tuned from 0.04 to 0.74 nm corresponding to heating width ranging from 1.000 to 3.750 mm.

In order to further broaden the bandwidth of the transmission peak, we propose to heat two adjacent local regions of the LCFBG with optimized conditions. The transmission peaks introduced by the two heating regions will combine into a broader transmission peak if the separation between the two heating regions is well controlled by the digital circuit, as shown in Fig. 8. $L_1$ and $L_2$ are the widths of the two heating local regions, respectively, and $\Delta L$ is the separation. Under the condition that $L_1$, $L_2$ and $\Delta L$ are set as 3.750, 0.750, and 0.500 mm, respectively, the 3-dB bandwidth of the transmission peak is broadened from 0.74 to approximately 1.55 nm (see the purple line in Fig. 9). If $\Delta L$ is bigger than 0.500 mm, the combined transmission peak will split. On the contrary, if

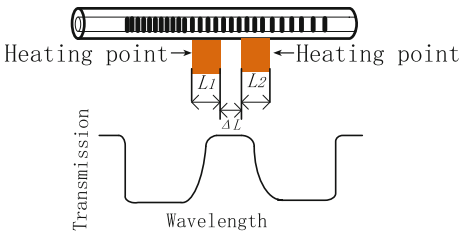


**Fig. 8** Principle of broadening the bandwidth by heating two adjacent regions

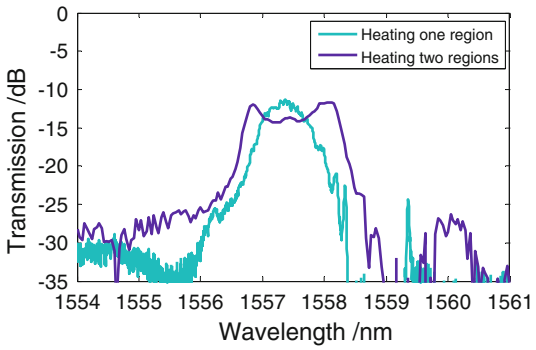


**Fig. 9** Transmission spectrum for heating two adjacent regions

$\Delta L$ decreases, the bandwidth of the transmission peak will certainly be narrower than 1.55 nm.

### 3.3 Multi-wavelength filtering performance

Having the relationship between the central wavelength of the transmission peaks and the heating local positions as expressed by Eq. (6), we can easily open a transmission channel with arbitrary central wavelength by heating the corresponding local region. What's more, multiple transmission channels can be obtained by heating multiple regions at the same time. The wavelength spacing between adjacent channels can be tuned flexibly through changing the distance between the two heating local regions. For instance, dual-wavelength filtering can be realized by heating two local regions simultaneously. Figure 10 shows the transmission spectrum of dual-wavelength filtering performance. The channel spacing between two peaks is 0.91 nm. The distance between two heating regions is 2.500 mm, and both heating widths are 0.750 mm. If the distance is shorter than 2.500 mm, the two peaks will affect each other. Improving the thermal contact between the LCFBG, the TPH and the heat sink will result in a better heat dissipation to remove the unwanted heat diffusion thus further decreasing the minimum channel spacing.

By heating three local regions along the LCFBG simultaneously, three transmission peaks were obtained, as

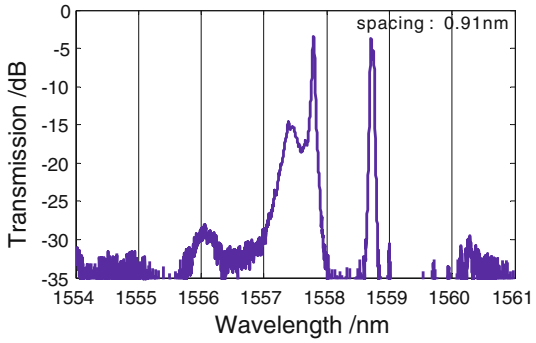


**Fig. 10** Transmission spectrum of the flexible filter with two peaks separated by 0.91 nm

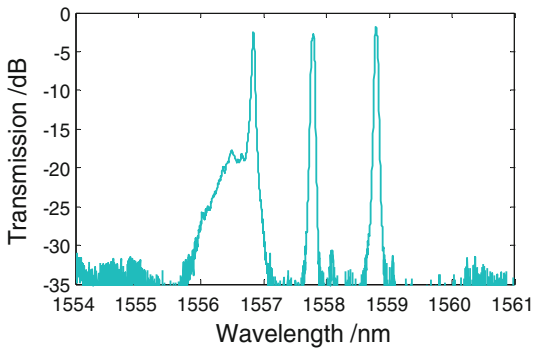


**Fig. 11** Transmission spectrum for three wavelengths filtering

shown in Fig. 11. The minimum insertion loss is about 1.76 dB, and the variation of transmitivity among channels is $< 1$ dB. By combining the above-mentioned technique, multiple channels with independently controlled bandwidth and spacing can be achieved.

## 4 Conclusions

In this paper, we have proposed and demonstrated a programmable all-fiber structured waveshaper based on a LCFBG and a TPH. The key parameters of this filter such as the number of transmission channels, passing bandwidth per channel, central wavelength as well as the channel spacing can be reconfigured independently and flexibly by a program-controlled circuit. The central wavelength of the transmission channel can be tuned from 1,547.16 to 1,558.64 nm, the tunable passing bandwidth is tunable from $< 0.04$ to 1.55 nm, and the minimum channel spacing in multi-wavelength operation condition is 0.91 nm. In the experiments, an insertion loss of about 1.76 dB and a sideband suppression ratio of about 28 dB have been obtained. Improving the thermal contact between the LCFBG, the TPH and the heat sink will be helpful to produce the best possible results of this fully digital-controlled device for many optical applications.

**Acknowledgments** This work is supported by the National Natural Science Foundation of China (Grant No. 61107087) and the National High-tech R&D Program of China (863 Program) (Grant Nos. SS2012AA010407 and 2013AA010502).

## References

1. C. Raffaelli, M. Savi, ICTON, Tu.A1.3 (2012)
2. N. Amaya, M. Irfan, G. Zervas, K. Banias, M. Garrich, I. Henning, D. Simeonidou, Y.R. Zhou, A. Lord, K. Smith, V.J.F. Rancano, S. Liu, P. Petropoulos, D.J. Richardson, ECOC, Th.13.K.1 (2011)
3. D. Sinefeld, D.M. Marom, OFC/NFOEC technical digest, paper: OW1C.6 (2012)
4. WaveShaper Family Product Brochure. http://www.finisar.com/products/optical-instrumentation
5. T. Erdogan, J. Lightwave Technol. **15**, 1227–1294 (1997)
6. H.P. Li, X.X. Chen, J. Lightwave Technol. **28**, 2017–2022 (2010)
7. X.X. Chen, L.L. Xian, K. Ogusu, H.P. Li, IEEE Photon. Technol. Lett. **23**, 498–500 (2011)
8. S.Y. Li, N.Q. Ngo, S.C. Tjin, L.N. Binh, Opt. Commun. **239**, 339–344 (2004)
9. S.Y. Li, N.Q. Ngo, S.C. Tjin, P. Shum, J. Zhang, Opt. Lett. **29**, 29–31 (2004)
10. Q. Ngo, D. Liu, S.C. Tjin, X.Y. Dong, P. Shum, Opt. Lett. **30**, 2994–2996 (2005)
11. N.Q. Ngo, S.Y. Li, L.N. Binh, S.C. Tjin, Opt. Commun. **260**, 428–441 (2006)
12. I. Petermann, S. Helmfrid, O. Gunnarsson, L. Kjellerg, J. Opt. A: Pure Appl. Opt. **9**, 1057–1061 (2007)
13. S. Takahashi, S. Shibata, J. Non-Cryst, Solids **30**, 359–370 (1979)